PREVISÃO DE ESTRESSE TÉRMICO E ADESÃO NO SISTEMA DE REVESTIMENTO NÃO CANÔNICO

FORECASTING OF THERMAL STRESS AND ADHESION IN NON-CANONICAL SUBSTRATE – COATING SYSTEM

ПРОГНОЗИРОВАНИЕ ТЕРМИЧЕСКИХ НАПРЯЖЕНИЙ И АДГЕЗИИ В НЕКАНОНИЧЕСКОЙ СИСТЕМЕ ПОКРЫТИЯ

ASTAPOV, Alexey N.[1]; NUSHTAEV, Dmitry V.[2*]; RABINSKIY, Lev N.[1]

[1] Moscow Aviation Institute (National Research University), Department of Advanced Materials and Technologies of Aerospace Application, 4 Volokolamskoe shosse, zip code 125993, Moscow – Russian Federation
(phone: +7 499 158 42 64)

[2] TESIS Limited Liability Company, Department of Design and Engineering Analysis, 18 Yunnatov Str., zip code 127083, Moscow – Russian Federation
(phone: +7 495 612 44 22)

** Corresponding author*
e-mail: nyshtaev.vfb@rambler.ru

Received 30 June 2018; received in revised form 15 November 2018; accepted 05 December 2018

RESUMO

O modelo matemático é baseado na análise FE para avaliar o estado de tensão-deformação sob a carga térmica do sistema de revestimento do substrato, levando em consideração as características de deformação não-canônica do substrato. O problema da termoelasticidade foi resolvido para o estado generalizado deformado no sistema de CAE SIMULIA Abaqus. Distribuição desigual de tensões térmicas no sistema é obtida em torno do perímetro do perfil da lâmina. Com base na tecnologia de superfície coesiva, foi desenvolvido um método para calcular a tensão de contato padrão e tensão tangencial de superfície, que iniciam a descontinuidade do adesivo no sistema de revestimento do substrato. Apresenta-se a avaliação do nível de aderência exigido do substrato e revestimento, garantindo a integridade do sistema em determinadas condições de operação. A atualização dos resultados obtidos é realizada tendo em consideração as deformações plásticas irreversíveis da camada de revestimento a diferentes temperaturas. É mostrado que o aparecimento de deformações inelásticas do revestimento afeta significativamente o nível de tensões térmicas e residuais em todo o sistema, bem como o nível de tensão de contato na interface entre o substrato e o revestimento iniciando a quebra do adesivo. Previsão do nível de estresse e sua distribuição, bem como a força de aderência em sistemas de revestimento, aplicam uma abordagem cientificamente fundamentada no desenvolvimento de uma arquitetura de revestimento (camada química e de fase, sua quantidade, espessura e métodos de formação) e reduzem significativamente o número de testes experimentais, seu tempo e custos.

Palavras-chave: *tensões resistentes ao calor, revestimentos funcionais, resistência adesiva, superfície coesiva, modelo elástico.*

ABSTRACT

The mathematical model is constructed on the basis of FE-analysis for evaluation of stress-strain state under a thermal load of substrate – coating system considering non-canonical substrate deformation features. The simply connected thermoelasticity problem is solved for generalized plane strain state in CAE-System SIMULIA Abaqus. Nonuniform distribution of thermal stresses in the system is obtained along the perimeter of

DOI: 10.52571/PTQ.SI1.2018.465_PeriodicoES.pdf

the blade profile. Based on cohesive surface technology the technique was developed for calculation of standard and shear contact stress level, initiating an adhesive fracture in the substrate - coating system. The estimation of the required substrate and coating adhesion strength level securing the system integrity under specified operating conditions is proposed. The updating of the obtained results is performed taking into account the coating layer's irreversible plastic deformations under different temperatures. It's shown that the appearance of coating inelastic deformations significantly influences on the level of thermal and residual stresses in the whole system as well as contact stress level at the interface substrate – coating initiating adhesive violation. The prognosis of stress level and distribution, as well as adhesive strength in the substrate – coating systems, allow scientifically approaching to the development of coating architecture (chemical and phase layer composition, its number, thickness and formation methods) and significantly decreases the number of experimental tests, their time and costs.

Keywords: *heat induced stresses, functional coatings, adhesion strength, cohesive surface, elastic model*.

АННОТАЦИЯ

Построена математическая модель на основе МКЭ для оценки напряженно-деформированного состояния при тепловом нагружении системы подложка – покрытие с учетом особенностей деформирования подложки неканонической формы. Решена односвязная задача термоупругости в постановке для обобщенной плоской деформации в CAE-системе SIMULIA Abaqus. Получено неравномерное распределение тепловых напряжений в системе по периметру профиля лопатки. На основе технологии cohesive surface разработана методика определения уровня нормальных и сдвиговых контактных напряжений, инициирующих адгезионное разрушение в системе подложка - покрытие. Дана оценка требуемого уровня прочности сцепления покрытия с подложкой, обеспечивающего сохранение целостности системы в рассмотренных условиях эксплуатации. Проведено уточнение полученных результатов посредством учета возможности образования необратимых пластических деформаций в слое покрытия при различных температурах. Показано, что возникновение неупругих деформаций в покрытии существенным образом влияет на уровень тепловых и остаточных напряжений во всей системе, а также на уровень контактных напряжений на границе раздела подложка - покрытие, инициирующих нарушение адгезии. Прогнозирование уровня, характера распределения напряжений и адгезионной прочности в системе подложка - покрытие позволяет научно подойти к разработке архитектуры покрытий (химического и фазового состава слоев, их количества, толщин и способов формирования) и значительно сократить объем экспериментальных испытаний, время и затраты на них.

Ключевые слова: *теплоустойчивые напряжения, функциональные покрытия, адгезионная прочность, когезионная поверхность, эластичная модель*.

INTRODUCTION

The demand for structural materials capable of operating in aggressive environments under pressure and high temperatures increases with technology development (Formalev *et al.*, 2018; Kolesnik *et al.*, 2015). Besides, even the best currently popular materials, having necessary mechanical strength, need to be provided with necessary functional properties (wear resistance, corrosive resistance, heat resistance, thermal stability, erosive mass loss resistance, catalytic activity etc.). These problems are solved basically with the help of thin-layer protective coatings (Appen, 1976; Hoking *et al.*, 2000; Bobrov *et al.*, 2014; Astapov, 2014; Astapov and Terent'eva, 2016; Astapov and Rabinskiy, 2016) on surfaces of parts contacting with the environment.

Moving from the main (bearing) material to the layered coating, property jump or gradient inevitably appears, particularly the coefficient of thermal (linear) expansion (CLE), as a result, internal stresses are appeared in multilayer systems (Appen, 1976; Bobrov *et al.*, 2014; Astapov and Nushtaev, 2016; Astapov and Zhavoronok, 2016; Astapov *et al.*, 2017). It leads to decrease in adhesive strength and increase of failure velocity in the operation process, particularly in places with a small curvature radius of the surfaces (on sharp edges, geometry change areas). The central issue of searching the coating optimal architecture is the relationship between the structural parameters of substrate - coating system (quantity and layer width), mechanical and thermal properties of layer materials with functional and operational system features (Silva *et al.*, 2017). The coating structure

parameters and its layer materials select criteria, as a rule, represents stress minimization (residual, thermal), appeared in multilayer system during its forming and operation.

The analysis of coating strain-stress state (SSS) on the flat substrate under thermal effect proved (Appen, 1976; Astapov et al., 2016; Astapov, and Zhavoronok, 2016; Astapov *et al.*, 2017) that compression stresses, exceeding the permissible limit, lead to coating layer separation or coating-substrate fracture while tensile stress – to cracks and micropores. The additional tensile or compressive forces acting normal to the surface (radial stresses) appear at substrates with curved coating layers. Besides, its influence result will depend primarily on the rate of CLE surface material layers and substrate and curvature type (concavity, convexity).

The analysis of SSS coatings on curved substrates of simple geometry (sphere, circular pipe) in momentless problem statement (neglecting bending deformations) is specified in (Appen, 1976; Sidorov *et al.*, 1966). Besides, in (Astapov and Nushtaev, 2016; Astapov and Zhavoronok, 2016; Astapov *et al.*, 2017) it is shown that the SSS investigation regardless of the bend section leads to unacceptable errors even in the simple case of the semi-infinite plate, aside from the curved substrate. Bending component contribution to the total SSS of multilayer systems especially increases when studying thin-walled structures, typical primarily of aviation and rocket and space equipment.

The Finite Elements Method (FEM) is widely used in the world practice to consider actual substrate geometry and sizes as well as its deformation peculiarities including bending effects. In particular, there is a large number of works in the domain of thermal barrier coating SSS modeling (Ahrens *et al.*, 2002; Sfar *et al.*, 2002; Bäker *et al.*, 2005; Białas, 2008; Hermosilla *et al.*, 2009; Ni *et al.*, 2011; Kahraman *et al.*, 2012; Yang *et al.*, 2014; Liu *et al.*, 2014; Han *et al.*, 2014), including cylindrical substrates (Ahrens 2002; Białas, 2002; Hermosilla *et al.*, 2009). The main focus is on the investigation of heat stress evolution in the process of operation as a result of diffusion formation at the interface “thermal barrier layer – heat-resisting layer”, so-called thermally-grown oxide. The used models consider the decisive effect of the unevenness of contact surface in the sphere of which the oxide layer appears and maximum stress concentration is realized. Works directed on SSS modeling of multilayer coatings on the non-canonical surface are not numerous (Kahraman et al., 2012;Yang et al., 2014; Liu et al., 2014), its results do not form finished methodology in the domain of investigation.

The other important quality parameter is the strength of its adhesion with the substrate (Bobrov *et al.*, 2014; Zimon et al., 1977; Lunev, and Nemashkalo, 2010). The performed analysis shows that the main methods being applied for adhesion indication are experimental procedures of direct coating separation from the substrate (on glue, sealed or pin method) (Bobrov et al., 2014; Zimon, 1977; Lunev and Nemashkalo, 2010; Zhu and Wlosinski, 2003; Liao et al., 2003) and scratching (sclerometry) (Lunev and Nemashkalo, 2010; Benjamin and Weaver, 1960; Hamilton and Goodman, 1966; Kinbara et al., 1999; Ichimura and Ishii, 2003; Sui and Cai, 2006). Besides, all tests are performed on plane sample surfaces, excluding the possibility of recording the real geometry features of multilayer structures on characteristics of adhesive layer strength.

The strength tests (Bobrov *et al.*, 2014; Zimon, 1977; Lunev and Nemashkalo, 2010; Zhu and Wlosinski, 2001; Pershin *et al.*, 2003; Liao *et al.*, 2003) are performed by stress creation at the interfaces between the coating layers and the main material. With that in mind the metal rods are glued or soldered to the coating surface, and then the tensile strength should be applied to it. The method disadvantage is a possibility of glue or solders penetration to the interface between the layers of coating and substrate and consequently, the possibility of changing the adhesive characteristics. Also, the statistics showed (Bobrov *et al.*, 2014; Zimon, 1977), that in the process of loading the separation often occurs not only on the interface but through the coating material. Such material damage is probably at low cohesion coating strength and presence or lack of adhesion in it. Usually, the destruction of the cylindrical joint starts from the periphery of the sample and then spreads to the rest of the area. The uneven destruction of the coating surface, conditioned by simultaneous action not only normal but partially shear stress does not allow obtaining true values of coating adhesive strength.

The Scratching Method (Lunev and Nemashkalo, 2010; Benjamin and Weaver, 1960; Hamilton, and Goodman, 1966; Kinbara *et al.*, 1999; Ichimura and Ishii, 2003; Gonczy and

Randall, 2005; Sui and Cai, 2006) is based on continuous coating loading by diamond indenter horizontally moving on a sample plane under continuous or increasing loading. The structure degradation analysis is indicated microscopically and also with the help of AE signal recording appearing in the process of layer scratching (Ichimura and Ishii, 2003). The scratching method is the most simple and fast method of qualitative evaluation of adhesive/cohesive coating behavior, so, it's widely used in practice, particularly in the process of comparative study performance. However, this method does not allow obtaining a true qualitative assessment of investigated parameters. As a rule, the cohesive strength of the coating is characterized by the value of the lower critical load on the indenter, at which layer scratching occurs with cracks. The upper critical load, at which coating or its separate layer begins fully flakes from the substrate or lower lying layers, corresponds to adhesion strength. A number of authors suppose simplified models (Benjamin and Weaver, 1960; Hamilton and Goodman, 1966; Kinbara *et al.*, 1999), allowing recalculate found critical load values to stresses, however, such calculation results give overestimated values of investigated characteristics, so, it can be used only for obtaining overestimated values.

FEM is the most appropriate tool for simulating crack formation and extension, layering growth in real multilayer structures due to its geometry complexity, load conditions and fastening. The analysis of the most common approaches to solving these problems (Astapov and Nushtaev, 2016; Białas, 2008; Rybicki and Kanninen, 1977; Belytschko and Black, 1999; Diehl, 2005; Nekkanty et al., 2007; Roth and Kuna, 2011; Kurochkin and Kozhina, 2012; Qin et al., 2012; Han *et al.*, 2016) showed that the cohesive surface represents the most practical technology for modeling multilayer coatings delamination process including high-temperature materials (Astapov and Nushtaev, 2016). The essence of the method consists of the additional contact layer introduction in the area of supposing fracture. The contact layer elasticity is formed based on the elasticity of contact elements according to mixture rule or set directly by the investigator. The crack appearance and opening in the system are controlled when the material achieves the adhesive layer of its strength limit which depends on the material strength of layers to be bonded. It's necessary to note that within these studies the great attention is paid to issues of modeling the processes of initiation and evolution of interlayer damage in the substrate – coating system (Astapov and Nushtaev, 2016; Białas, 2008; Nekkanty *et al.*, 2007; Roth and Kuna, 2011; Kurochkin and Kozhina, 2012; Qin et al., 2012; Han *et al.*, 2016). We have not found any works directly aimed at forecasting of coating layers adhesion strength characteristics and making connections between them and architecture of layer system.

So, the experimental evaluation of adhesive/cohesive coating characteristics allows performing control of its quality and optimizing manufacturing technological processes following such parameters as forming regimes, substrate surface preparation methods etc. However, in our opinion, the forecasting of examined coating quality parameters (residual stress, adhesive strength) is more logic procedure and some operational properties at early stages of material-technology solution acceptance. This will, on the one hand, allow scientifically approach to the development of coating architecture (selection of chemical and phase layer composition, its quantity, width and formation methods) and on the other hand, it will significantly decrease the experimental study and test volume and consequently, time and distribution costs. FEM should be used as a basic tool for modeling to the maximum approach of the simulation experiment to real operational conditions with coatings.

The aim of this work is the development of SSS analysis method of thin coating with the substrate of non-canonic form and determination of stress level initiating an adhesive fracture in layer systems. The work continues systematic author investigations, related to the development of functional protective coatings (Astapov, 2014; Astapov and Terent'eva, 2016; Astapov and Rabinskiy, 2017) and also the creation and development of mathematical models and methods (Astapov and Nushtaev, 2016; Astapov and Zhavoronok, 2016; Astapov *et al.*, 2017) and its SSS evaluation.

PROBLEM'S STATEMENT

In the present work, the coating will be considered within the integral structural wall with a protective material, representing the multilayer package substrate – coating. Such a model allows varying the set of required system features due to material rational choice and change of composition, quantity, and width of the coating.

Each wall layer including the substrate will be modeled by the continuous, non-porous simple connected medium of finite thickness regardless of the peculiarities of its material real microstructure. Structural discontinuity (hetero-phase, the presence of inclusions, defects and etc.) will be indirectly considered via specified layer material property characteristics. It's supposed that the total coating layer width is at least one order less than the substrate width, i.e. the coating is represented as thin layer systems.

We will restrict ourselves to consideration of only one-layer heat-resistant coating. The latter is designed for protection from high-temperature gas corrosion of heat-resistant materials (for example, nickel alloys, alloy steel etc.) and extension of thermal-time intertissue in the oxygen-containing medium. In further studies, the summary of found results is planned to be performed concerning multilayer heat-resistant coating and distribute for other compositions.

The process of soft cooling of a free of other external forces and limits non-canonical substrate with the applied one-layer coating is considered. The initial and final temperature values are T_0 = 1200°C and T_κ = 20°C accordingly. The aviation gas-turbine engine blade (GTEB) represents as the non-canonical substrate, made of polycrystal heat-resistant nickel-alloy. The typical heat-resistant aluminide coating manufactured of Ni-20Cr-12Al-0,5Y system SDP-2 alloy is applied to its front face. Materials mechanical and temperature property dependencies within 20÷1200°C are specified in the following Table 1.

The temperature dependencies of modulus elasticity values $E(T)$ and true CLE $\alpha(T)$ are extracted from the work (Budinovsky *et al.*, 2011). To determine strength temperature dependencies $\sigma_b(T)$ and relative elongation at break $\delta(T)$ of the SDP-2 alloy is performed the approximation of experimental data within temperature 500÷1000°C and 700÷1000°C accordingly, extracted from the work (Kachanov and Tamarin, 2007) with its following extrapolation within 20÷1200°C. To determine Poisson ratio $\nu(T)$ temperature dependencies and materials yield offset $\sigma_{0,2}(T)$ the calculation test is performed with the following target value approximation. The property modeling is performed according to an equivalent to the work (Astapov and Lifanov, 2014) by thermodynamic calculation method of multi-component system equilibration – CALPHAD (CALculation of PHAse Diagrams) in JMatPro software package. Calculations were performed for alloys of the following chemical compositions mac. %: Ni-5,4Al-9,8Co-9,0Cr-1,5Mo-1,0Nb-2,6Ti-10,3W-0,18C-0,04Zr-0,025B and Ni-20Cr-12Al. Data approximation and extrapolation is performed by the regressive analysis based on MS Excel spreadsheet. Data fitting authenticity is specified in table 1 by determination coefficient R^2.

Initially, the system has uniform temperature field with T_0 = 1200°C. It's supposed that the structural wall is free ($\sigma_{ij} = \varepsilon_{ij} = 0$) at this temperature. This corresponds to the system state in the process of high-temperature annealing or operation. In the process of cooling, in the result of mutual restriction of layers temperature deformation appearing because of substrate and coating difference in CLE, thermal stresses appear in the system. The analysis of their level and change character depending on temperature we will perform on the basis of simple connected thermoelasticity problem solution. It's necessary to consider that the temperature field is set and homogenous at each point of the system. Otherwise, this temperature field is calculated based on thermal conductivity solution considering contact conditions at the boundary of system layers (temperature chemical and heat flow rate). Temperature change law from T_0 to T_κ should be linear.

The solution of thermoelasticity problem should be performed in 2D form, i.e. for one of the related aviation GTE blade cross-sections (Figure 1). The geometrical profile sizes: maximum distance between extreme points (chord) L_s = 70 mm; maximum altitude (width) h_s = 3.5 mm; leading-edge radius (edge) r_s = 0.34 mm. The coating is applied along the whole profile perimeter by a uniform layer of thickness h_l = 100 μm. Subscripts used in the notation of values relating to wall layers: *s* – *substrate*, *l* – *layer*.

The SSS calculation procedure development and distribution will be performed using FEM on the basis of SIMULIA Abaqus (Abaqus Theory Manual…, 2016) software application suite. Substrate and coating are designed as two separate geometrical objects. The adhesive relationship between them is

performed based on *cohesive surface technology (*Astapov and Nushtaev, 2016; Diehl, 2015; Nushtaev and Astapov, 2017*)*, supposing the definition of special contact interactions. The contact elasticity is formed on the basis of elasticity binding finite elements according to mixture rule. At the first work stage, the rigid deformation model determined by Hook-Duhamel law is intended for the description of mechanical substrate and coating material response. So, the contact connection is also elastic. At the second stage obtained results specification is performed through use of the elastoplastic model of coating material response. It should be noted that within this study SSS is calculated in order to forecast the most likely areas of adhesive bond destruction in the substrate – coating system. Direct crack nucleation process modeling and its further evolution is not the subject of this work. The authors have devoted a special study to these problems (Astapov and Nushtaev, 2016).

The construction of the finite element model is carried out regarding profile geometric symmetry relating OX axis. The corresponding boundary conditions are determined following the section boundary. Two-dimensional four-node finite elements of CPEG4R type (Astapov et al., 2017; Abaqus Theory Manual…, 2014) are used. They work in standard plain strain mode ($\varepsilon_z = \text{const}$). The coating is approximated on width by five finite elements. In the vicinity of the adhesive layer on the side of the substrate and blade profile edge has used the technique of local mesh condensation of the FE model (Figure 2).

The temperature property dependencies of wall layer material properties $E(T)$, $\nu(T)$, $\alpha(T)$ (Table 1) will lead to change system rigidity matrix during the calculation, i.e. to material nonlinearity. With that in mind, the Incremental-Iterative (Newton-Raphson) (Abaqus Theory Manual…, 2016) is selected as nonlinear problem solution method being the base of Abaqus/Standard solver. The fixed temperature increment of ΔT = 20°C is selected.

SSS ASSESSMENT IN THE SUBSTRATE – COATING SYSTEM:

Based on the constructed finite element model the values of thermal stresses in the substrate were calculated when the structural wall cooling down. In Figure 3 the distribution of the main stresses in the system is shown at $T_к$ = 20°C. In the body of the blade, tensile residual stresses are fixed and compressive stresses are in the coating. Also in the figure control points along profile perimeter are marked which will be used for further analysis of the SSS system. All points are located at the boundary of section between the substrate and coating, i.e. in the adhesive layer of the system: *A* and *G* points – accordingly on high and low profile coating on the axis of its symmetry; *B* and *F* – intermediate points on flat profile sections; *C* and *E* – points of transition of profile flat part to curvilinear and back (beginning and end of the edge); *D* – edge peak.

In Figure 4 graphs of the distribution of the main stresses in the adhesive layer ($T_к$ = 20°C) along the profile perimeter, measured in *layer joints* and *substrate* directly close to the section boundary. At sections, *AB*, *BC,* and *GF*, *FE* the monotonic decrease of compressing stress are observed in the coating, in the substrate – an increase of tensile stresses. While moving from the profile symmetry axis and approaching the blade edge the stress rate increases. At points, *C* and *E* stress jumps can be found that is connected with the blade radius of profile curvature change. At the edge peak (point *D*) the coating drop is maximum and is equal $\Delta\sigma_l^-$ = 34 MPa. The maximum of tensile stresses in the substrate falls on points *C* and *E* σ_s^+ ≈ 56 MPa, further following the radius of edge stresses are decreased up to σ_s^+ ≈ 44 MPa. Based on the found distribution character of residual stresses, the temperature dependences of thermal stresses in system layers should be studied in points *A*, *C* and *D*.

The nature of the temperature stress dependence in coating and substrate at the boundary of its section in points *A*, *C,* and *D* of blade profile is shown in Figure 5 and Figure 6 accordingly. In order to narrow in the process of cooling the coating is supported by the substrate ($\alpha_s < \alpha_l$ at 137.6°C < T ≤ 1200°C), as a result, there is a tensile stress deformation, compensating temperature narrowing. So, the initial cooling stage corresponds to an intensive growth of tensile stress in the coating and compressing in the substrate. Its maximum values they obtain at temperature T ≈ 500°C, which is intended for coating σ_l^+ = 228.9 MPa

(point *A*), σ_l^+ = 196.4 MPa (point *C*) and σ_l^+ = 188.4 MPa (point *D*); for substrate – σ_s^- = –13 MPa (point *A*), σ_s^- = –58.2 MPa (point *C*) and σ_s^- = –49.2 MPa (point *D*). The following cooling leads to decrease of σ_l and σ_s. At T = 137.6°C the system is free of thermal stresses $\sigma_l = \sigma_s = 0$, because $\alpha_s = \alpha_l$. After T < 137.6°C ($\alpha_s > \alpha_l$) the increase of compressing in covering and tensile stresses are observed in the substrate. These stresses are achieved to the following values at T = 20°C accordingly σ_l^- = –203.4 MPa (point *A*), σ_l^- = –176.9 MPa (point *C*) and σ_l^- = –169.2 MPa (point *D*); σ_s^+ = 11.6 MPa (point *A*), σ_s^+ = 53.3 MPa (point *C*) and σ_s^+ = 44.4 MPa (point *D*). Such behavior can be explained by complicated CLE dependencies and mechanical characteristics of layer materials from the temperature (Table 1).

It should be noted that found stress values at the point *A* on the flat profile section at the site of its maximum altitude are well correlated with the results of analytical calculations (Astapov *et al.*, 2017; Nushtaev and Astapov, 2017), executed by us within widely used in practice momentless approximation of SSS assessment of multilayer systems (Appen, 1976; Budinovsky *et al.*, 2011). When going from flat profile sections to curved ones (points C and D) we can see a decrease in the general level of thermal stress in the coating. The marked difference achieves its maximum value at temperature T ≈ 500°C and is equal approximately 40 MPa. For the substrate the situation changes in the opposite direction – edge stresses multiply exceed stress values at the point *A*. Such behavior is related to the increase of bending deformation contribution and curve when going from flat profile sections to curvilinear ones and simultaneous decrease of substrate width (Figure 3).

Also, a significant gradient change is found on coating width depending on the position of blade profile studying section. Thus, the gradient of residual stresses on width at the point *A* at T_κ = 20°C is about 0.1 MPa and at the point *D* – about 40 MPa.

EVALUATION OF ADHESIVE BOND IN THE SUBSTRATE – COATING SYSTEM:

As noted in p. 2, the adhesive bond between substrate and coating is modeled based on contact interaction with the introduction of elastic rigidity between contact coatings. The state evaluation of adhesive bond is comfortable to be performed depending on the level of contact stress in the substrate – coating system. They are divided into normal and shear components. Normal contact stresses *(CPRESS)* act normally to contact surfaces. Positive value normally corresponds to the compression of contact surfaces and negative value leads to its detachment. The contact shear *(CSHEAR)* characterizes the work of contact surfaces for shear (relative movement). So, in the area of negative values normal *CPRESS* coating detachment should be expected (*Mode I*: fracture for detachment) and in the areas of maximum *CSHEAR* meanings – tangentially (*Mode II*: fracture for shear).

In Figure 7 and Figure 8, the graphs of normal and shear contact stress distribution in the adhesive bond between substrate and coating are shown along the profile perimeter of investigating GTE blade at T_κ = 20°C. In sections *AC* and *GE* the values *CPRESS* and *CSHEAR* have about-zero values. With that in mind, the destruction of adhesive bond on flat profile blade sections is hardly probable. When going to the blade edge the significant value increase of normal contact stresses with a negative sign can be seen that suggests on potential possibility of surface detachment from the substrate surface. *CPRESS* variable achieves its maximum value at the edge top (in point *D*) and reaches a value of 43 MPa. *CSHEAR* value undergoes the jump in points *C* and *E* (edge beginning and end) and achieves values of 17.7 MPa.

Figure 9 shows normal and shear contact stresses temperature dependences in points *D* and *E*, where corresponding variables maximums are marked. If T > 137.6°C ($\alpha_s < \alpha_l$) the variable *CPRESS* shall be positive, i.e. coating surface compresses the substrate surface that normally prevents the destruction of the adhesive bond (failure). If T < 137.6°C ($\alpha_s > \alpha_l$) *CPRESS* shall change its sign that creates the basis for possible failure of the coating. The variable *CPRESS* achieves its maximum value at full wall cooling up to T_κ = 20°C and is 43 MPa. The sign of shear contact stress variable (*CSHEAR*) does not have any role when evaluating the possibility of fracture of adhesive bond for sheer – high priority

has a module of this variable. The maximum of *CSHEAR* variable is for the temperature of T ≈ 500°C and equal to 18.7 MPa. So, the adhesive bond fracture for shear mostly obvious at this temperature (T ≈ 500°C) but not at the final cooling stage $T_к$ = 20°C.

COATING MATERIAL ELASTIC-PLASTIC DEFORMATION ACCOUNTING:

In the previously considered problems for the description of substrate and coating material mechanical response the elastic behavior model has used regardless of the possibility of formation of elastic-plastic zones. However, according to the found results in p. 3, the stretching thermal stresses when cooling in the coating SDP-2 at *T* > 700°C exceed the yield point of the material (see Figure 5 and Table 1). This fact indicates on the applicability of elastic-plastic model for the description of coating material behavior. For the description of substrate material JC6U the elastic model is sufficient to be restricted because the level of developing thermal stresses in it is lower than the agreed material yield point within the whole temperature range (Figure 6 and Table 1).

To describe the mechanical response of the material the elastic-plastic model was selected with isotropic hardening (Abaqus Theory Manual…, 2016). The model uses the Mises yield surface and the associated law of plastic flow. Due to an insufficient quantity of experimental data the elastic-plastic area of deformation diagram is represented as a linear dependence $\sigma(\varepsilon)$. The control points of this diagram as follows: yield limit $\sigma_{0,2}$; strength σ_b and maximum deformation at the break δ. The temperature dependences of specified parameters (Table 1) are recorded.

In the result of performed calculations, it was found that the coating material works inelastic – plastic domain. The initialization moment of elastic-plastic material deformation of the coating corresponds to T = 1175°C. After cooling up to T = 905°C the growth of equivalent plastic deformation ε^{pl} stops, that caused by the increase of $\sigma_{0,2}$ with decrease of current temperature. Figure 10 describes the distribution of the principal plastic strains in the coating layer along the blade profile perimeter at the final temperature $T_к$ = 20°C. Compressing plastic deformations are marked along the whole perimeter. They achieve its maximum values (0.072 %) in points *A* and *G*.

The occurrence of irreversible plastic deformations in the coating changes the level of thermal stresses in the system as a whole. The accounting of elastic-plastic deformation leads to the expected increase of compressing stresses in the coating layer at full cooling to $T_к$ = 20°C comparing to the results found when using the material behavior elastic model (Figure 11). The mean growth level of compressing stresses in the coating along the blade profile perimeter is $\Delta\sigma_l$ ≈ 80 MPa. The mean increase of tensile stresses is noted in the substrate of $\Delta\sigma_s$ ≈ 11 MPa (Figure 12).

Figure 13, 14 show the influence of elastic-plastic material deformation accounting on values of normal and shear contact stresses in adhesive bond. Except for the final stage of cooling, it's noted the decrease of level both normal and shear contact stresses in the domain of high and medium temperatures. However, the maximum stress level increased from 43 to 59 MPa for *CPRESS* and from 18.7 to 22 MPa for *CSHEAR*. Variables maximum values correspond to the full cooling temperature of the structure wall $T_к$ = 20°C.

So, based on the performed level evaluation of normal and shear contact stresses in adhesive bond for selected GTE blade configuration and accepted layer material properties the adhesive system strength substrate – coating at break should exceed the value of 59 MPa and for shear 22 MPa.

CONCLUSIONS:

1. The mathematical model was developed based on FEM for evaluation of SSS of substrate – coating system under thermal loading considering the peculiarities of non-canonical substrate deformation. The once coupled thermoelasticity problem was solved for the generalized plane strain state in CAE-system SIMULIA Abaqus. GTE aviation blade was considered as a non-canonical substrate. Non-uniform distribution of thermal stresses in the system along the perimeter of the blade profile is obtained. At transition points of flat profile sections to curvilinear ones (to the edge), stress jumps are found.

2. The domain of applicability of analytical momentless model widely used in practice is defined in the process of stress evaluation in the substrate – coating system – rectilinear, substrate plateau relating to a relatively large thickness. When investigating the stress-strain state of complex multilayer thin-walled structures the influence of bending deformation and system deformation is significant. In the area of the blade edge, a significant stress gradient is found on coating layer thickness, which is absent on flat system sections.

3. Based on *cohesive surface technology* the technique was developed for calculation of standard and shear contact stress level, initiating an adhesive fracture in the substrate – surface system. The most probable areas and temperatures of fracture initiation of adhesive bond stress and shear are calculated for selected blade configuration and accepted substrate material properties. The estimation of the required substrate and coating adhesion strength level is specified. It secures system integrity under specified operating conditions.

4. The obtained results were refined by taking into account the possibility of irreversible plastic deformations in the coating layer at different temperatures. The associated flow law considering von Mises yield condition is used for the description of elastic-plastic material behavior. It's shown that the appearance of coating inelastic deformations significantly influences on the level of thermal and residual stresses in the whole system as well as contact stress level at the interface substrate – coating system initiating adhesive violation.

5. The forecasting of the level, stress distribution and adhesive strength in the substrate – coating system allows scientifically approaching to the development of coating architecture (chemical and phase layer composition, its number, thickness and formation methods) as well as significantly decrease the number of experimental tests, their time and costs. The database on physical and mechanical and thermal properties of laminate materials should be created for the performance of a specific evaluation of the thermal and stress-strain behavior of different functional coatings.

ACKNOWLEDGMENT:

This work is executed at Moscow Aviation Institute with financial support from RSF within the award "Execution of fundamental scientific researches and exploration research activities by international scientific groups". President's program on investigation activities (Agreement No 17-79-10325 of 25.07.2017).

REFERENCES:

1. Abaqus Theory Manual. USA: Dassault Systemes Simulia Corp., Providence, RI, 2016. Available at: https://www.researchgate.net/profile/Dossa_Boko-Haya/post/Where_can_I_get_abaqus_online_tutorials_that_are_detailed_enough_to_work_through_them_without_additional_assistance/attachment/59d6412cc49f478072eaab5f/AS%3A273794676002816%401442289145057/download/9_Abaqus-cae-Users-Theories_Manual.pdf
2. Ahrens, M., Vaßen, R., Stöver, D. *Surface and Coatings Technology*, **2002**, *161(1)*, 26 – 35. DOI: 10.1016/S0257-8972(02)00359-6.
3. Appen, A.A. *Temperature-resistant inorganic coatings*. Leningrad: Khimiya, **1976**.
4. Astapov, A.N. *Nanomechanics Science and Technology: An International Journal*, **2014**, *5(4)*, 267-285. DOI: 10.1615/NanomechanicsSciTechnolIntJ.v5.i4.20.
5. Astapov, A.N., Lifanov, I.P. Thermodynamic calculation of mechanical and thermophysical properties of austenitic steel at high temperatures. *Abstracts of the International Scientific Seminar "Dynamic deformation and contact interaction of thin-walled structures under the influence of fields of different physical nature",* Moscow: MAI, **2014**.
6. Astapov, A.N., Nushtaev, D.V. Calculation of thermal stresses in a substrate – coating system. *Materials of XXII International symposium "Dynamic and technological issues of structural mechanics and continuum" by A.G. Gorshkov.* Moscow: LLC "TP-print", **2016**.
7. Astapov, A.N., Nushtaev, D.V., Rabinskiy, L.N. *Composites: Mechanics, Computations, Applications. An International Journal*, **2017**, *8(4)*, 267-286. DOI: 10.1615/CompMechComputApplIntJ.v8.i4.10.

8. Astapov, A.N., Rabinskiy, L.N. *Solid State Phenomena*, **2017**, *269*, 14 – 30. DOI: 10.4028/www.scientific.net/SSP.269.14.

9. Astapov, A.N., Terent'eva, V.S. *Russian Journal of Non-Ferrous Metals*, **2016**, *57(2)*, 157-173. DOI: 10.3103/S1067821216020048.

10. Astapov, A.N., Zhavoronok, S.I. Calculation of SSS in a multi-layer «substrate – functional coating» system under thermal loading. *Proceedings of the Second International Conference Deformation and Failure of Composite Materials and Structures (DFCMS-2016)*. Moscow: Stolitsa, **2016**.

11. Bäker, M., Rösler, J., Heinze, G. *Acta Materialia*, **2005**, *53(2),* 469-476. DOI: 10.1016/j.actamat.2004.10.004.

12. Belytschko, T., Black, T. *International Journal for Numerical Methods in Engineering*, 1999, 45(5), 601-620. DOI: 10.1002/(SICI)1097-0207(19990620)45:5<601::AID-NME598>3.0.CO;2-S.

13. Benjamin, P., Weaver, C. *Proceedings of the Royal Society A*, **1960**, 254(1277), 163-176. DOI: 10.1098/rspa.1960.0012.

14. Białas, M. *Surface & Coatings Technology*, **2008**, *202*, 6002-6010. DOI: 10.1016/j.surfcoat.2008.06.178.

15. Bobrov, G.V., Ilin, A.A., Spektor, V.S*. Theory and technology of formation of inorganic coatings.* Moscow: Alfa, **2014**.

16. Budinovsky, S.A., Kablov, E.N., Muboyadzhyan, S.A. *Bulletin of Bauman Moscow State Technical University. Series: Engineering*, **2011**, *SP2*, 26 -37.

17. Diehl, T. Modeling surface-bonded structures with ABAQUS cohesive elements: beam-type solutions. *Proceedings of the ABAQUS User's Conference 2005. May 18-20, 2005, Stockholm, Sweden*, **2005**. Available at: http://www.2kornucopia.com/pdfs/Diehl_Elastic_Cohesive_element_AUC2005.pdf

18. Formalev, V.F., Kolesnik, S.A., Kuznetsova, E.L. *High Temperature*, **2018**, *56(3)*, 393-397.

19. Gonczy, S.T., Randall, N. *International Journal of Applied Ceramic Technology*, **2005**, 2(5), 422-428. DOI: 10.1111/j.1744-7402.2005.02043.x.

20. Hamilton, G.M., Goodman, L.E. *Journal of Applied Mechanics*, **1966**, 33(2), 371 – 376. DOI: 10.1115/1.3625051.

21. Han, B., Veidt, M., Reiner, J., Dargusch, M. *Journal of Mechanical Engineering Research*, **2016**, *8(1)*, 1-17. DOI: 10.5897/JMER2015.0377.

22. Han, M., Huang, J., Chen, S. *Ceramics International*, **2014**, *40(2)*, 2901-2914. DOI: 10.1016/j.ceramint.2013.10.021.

23. Hermosilla, U., Karunaratne, M.S.A., Jones, I.A., Hyde, T.H., Thomson, R.C. *Materials Science and Engineering: A,* **2009**, *513-514*, 302-310. DOI: 10.1016/j.msea.2009.02.006.

24. Hoking, M., Vasantasri, V., Sidki, P. *Metallic and Ceramic coatings: manufacture, properties, and application*. Moscow: Mir, **2000**.

25. Ichimura, H., Ishii, Y. *Surface and Coatings Technology*, **2003**, 165(1), 1-7. DOI: 10.1016/S0257-8972(02)00718-1.

26. Kachanov, E.B., Tamarin, Y.A. *Technology of light alloys*, **2007**, *1*, 140-148.

27. Kahraman, Y., İriç, S., Taymaz, İ. *TOJSAT – The Online Journal of Science and Technology*, **2012**, 2(2), 51-56.

28. Kinbara, A., Baba, S., Kusano, E. Adhesion measurement of thin films on glass substrates by the scratch method. *Proceedings of the 2nd International Conference on Coatings on Glass (ICCG-2)*. Saarbrucken: Elsevier, **1999**.

29. Kolesnik, S.A., Formalev, V.F., Kuznetsova, E.L. *High Temperature*, **2015**, *53(1)*, 68-72.

30. Kurochkin, A.V., Kozhina, T.D. *Bulletin of the Solovyov Rybinsk State Aviation Technological Academy*, **2012**, *2*, 23-28 (in Russian).

31. Liao, Y.-d., Li, Z.-y., Tang, G.-q. *Journal of Wuhan University of Technology – Mater. Sci. Ed.,* **2003**, 18(1), 31-36. DOI: 10.1007/BF02835083.

32. Liu, D., Kyaw, S.T., Flewitt, P.E.J., Seraffon, M., Simms, N.J., Pavier, M., Jones, I.A. *Materials Science and Engineering: A*, **2014**, *606*, 117-126. DOI: 10.1016/j.msea.2014.03.014.

33. Lunev, V.M., Nemashkalo, O.V. *Journal of Physics and surface engineering*, **2010**, *8(1)*, 64-71.

34. Nekkanty, S., Walter, M.E., Shivpuri, R. *Journal of Mechanics of Materials and Structures*, **2007**, 2(7), 1231-1247. DOI: 10.2140/jomms.2007.2.1231.

35. Ni, L.Y., Liu, C., Huang, H., Zhou, C.G. *Journal of Thermal Spray Technology,* **2011**, *20(5)*, 1133 – 1138. DOI: 10.1007/s11666-011-9647-8.

36. Nushtaev, D.V., Astapov, A.N. Analysis of SSS system «heat-resisting material – coating» relating to noncanonical substrate. *Materials of XXIII International symposium "Dynamic and technological issues of structural mechanics and continuum" by A.G. Gorshkov.* Moscow: LLC "TRP", **2017**.

37. Pershin, V., Lufitha, M., Chandra, S., Mostaghimi, J. *Journal of Thermal Spray Technology*, **2003**, *12(3)*, 370-376. DOI: 10.1361/105996303770348249.

38. Qin, F., Shen, N., Chou, K. Implementing a cohesive zone interface in a diamond-coated tool for 2D cutting simulations. *Proceedings of the ASME 2012 International Mechanical Engineering Congress and Exposition.* Houston: ASMA, **2012**.

39. Roth, S., Kuna, M. *Proceedings in Applied Mathematics and Mechanics*, **2011**, 11(1), 175-176. DOI 10.1002/pamm.201110079.

40. Rybicki, E.F., Kanninen, M.F. *Engineering Fracture Mechanics*, **1977**, 9(4), 931-938. DOI: 10.1016/0013-7944(77)90013-3.

41. Sfar, K., Aktaa, J., Munz, D. *Materials Science and Engineering: A*, **2002**, *333(1-2)*, 351-360. DOI: 10.1016/S0921-5093(01)01859-7.

42. Sidorov, A.B., Kulyamina, L.L., Zhornik, A.I. *Glass,* **1966**, *2*, 51-59.

43. Silva, M., Chaves, T.A.B.; Pacheco, R.R.; Goulart, A.C.; Santos, J.P.V., Goulart, S.M. *Periodico Tche Quimica*, **2017**, *14(28)*, 130-139.

44. Sui, J.H., Cai, W. *Nuclear Instruments and Methods in Physics Research Section B: Beam Interactions with Materials and Atoms*, **2006**, *251(2)*, 402-406. DOI: 10.1016/j.nimb.2006.06.028.

45. Yang, L., Liu, Q.X., Zhou, Y.C., Mao, W.G., Lu, C. *Journal of Materials Science & Technology*, **2014**, *30(4)*, 371-380. DOI: 10.1016/j.jmst.2013.11.005.

46. Zhu, S., Wlosinski, W. *Journal of Materials Processing Technology*, **2001**, 109(3), 277-282. DOI: 10.1016/S0924-0136(00)00814-1.

47. Zimon, A.D. Adhesion of films and coatings. Moscow: Chemistry, **1977**.

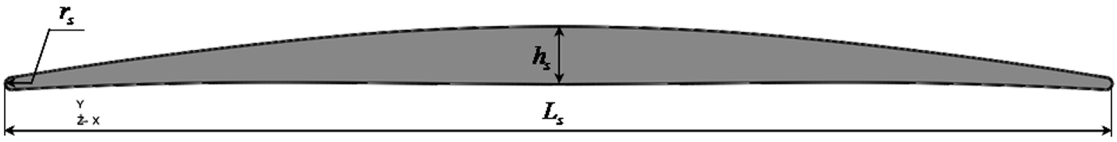

Figure 1. *Aviation GTE Blade Profile*

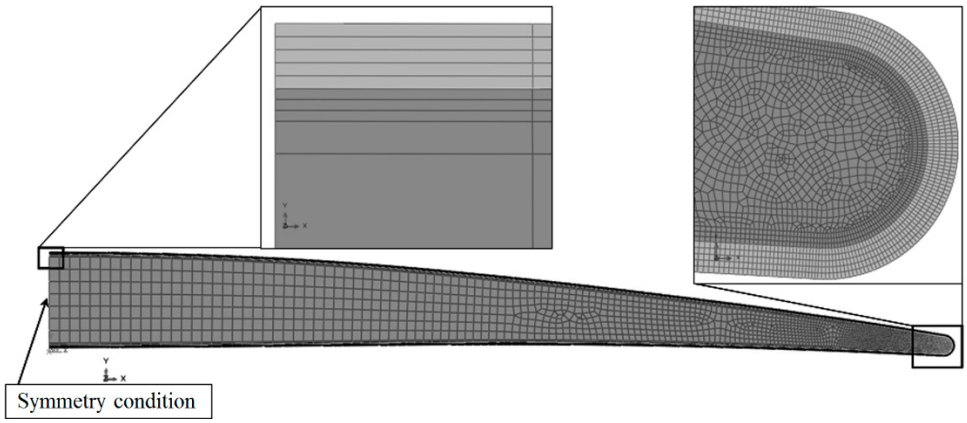

Figure 2. *FE model of the structural wall*

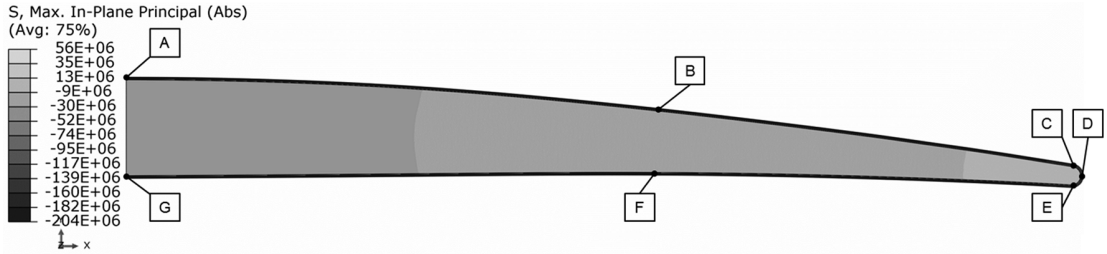

Figure 3. *Distribution of the main stresses at $T_к$ = 20°C, Pa and control point position along the profile perimeter*

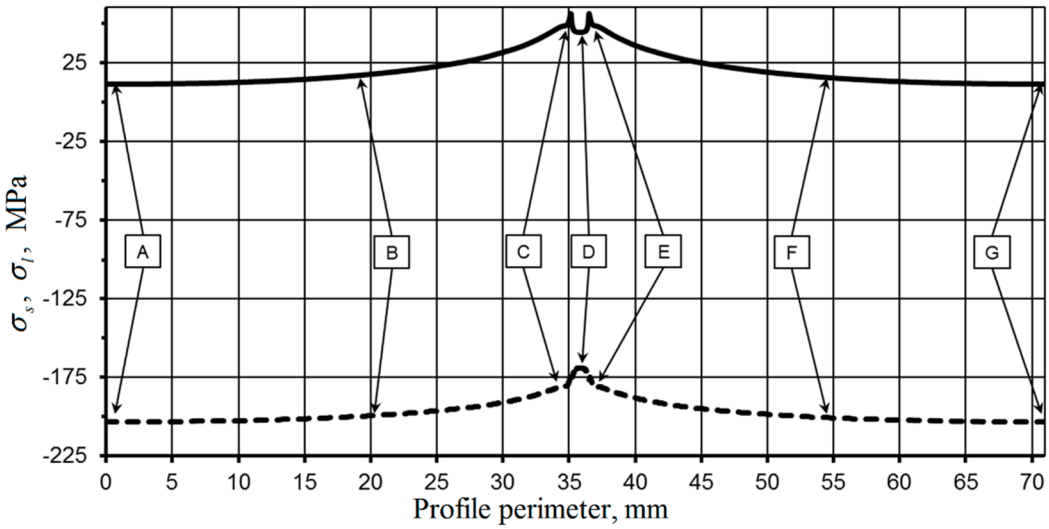

Figure 4. *Change of residual stresses at the section boundary substrate – coating along the profile perimeter, MPa:*
——– substrate; - - - - – coating

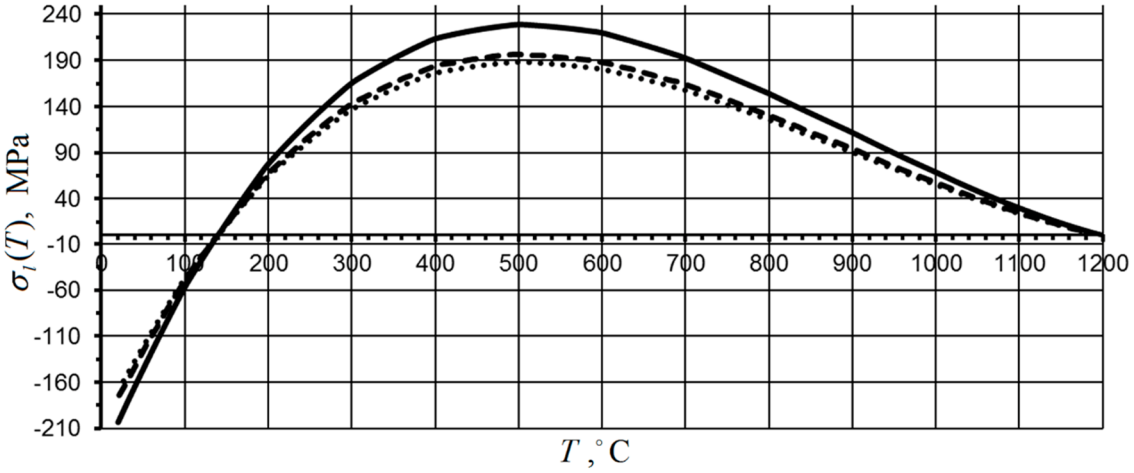

Figure 5.*Thermal stress temperature dependences in the coating, MPa:*
——– point A; – – – – point C; ····· – point D

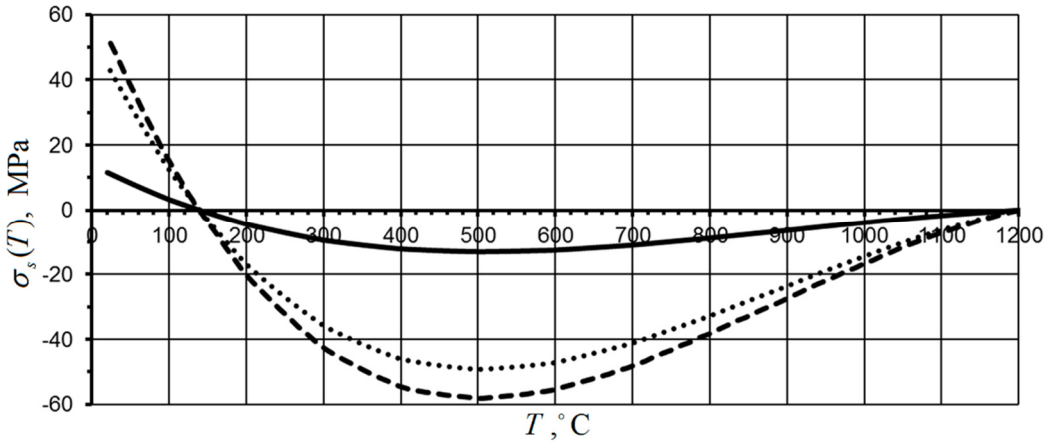

Figure 6. *Temperature dependences of thermal stresses in the substrate, MPa:*
——– point A; – – – – point C; ····· – point D

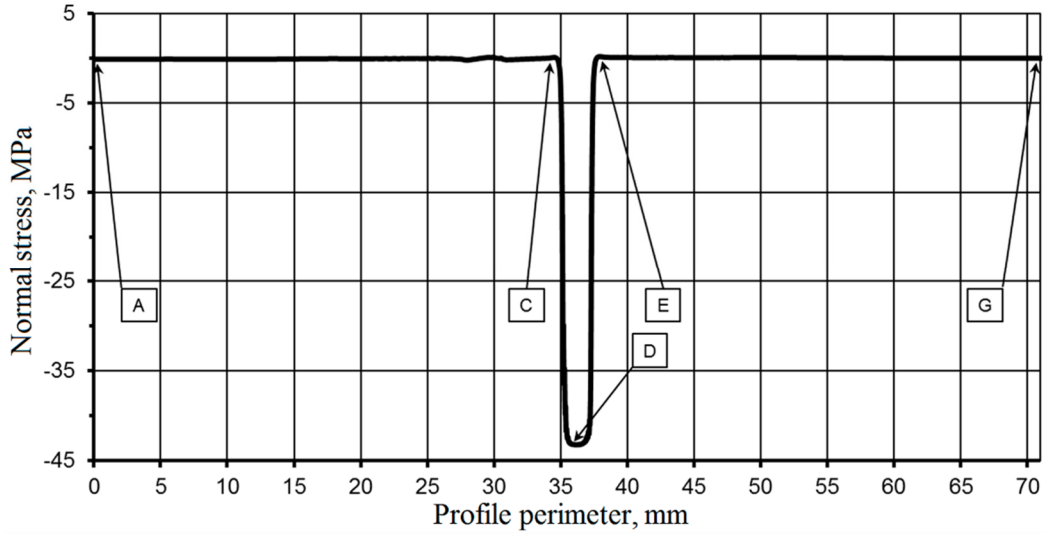

Figure 7. *Distribution of normal contact stresses CPRESS in the substrate – coating system along profile perimeter at* $T_к$ *= 20°C, MPa*

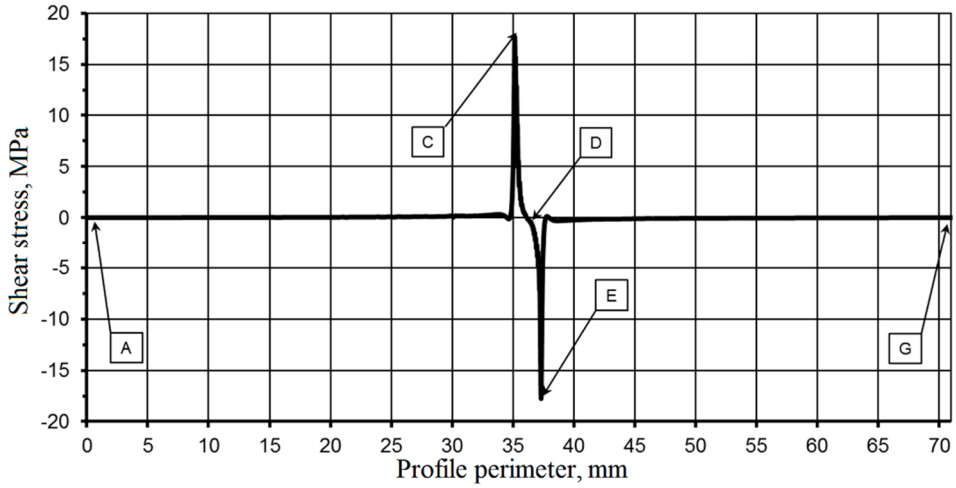

Figure 8. *Distribution of shear contact stresses CSHEAR in the substrate – coating system along profile perimeter at $T_к$ = 20°C, MPa*

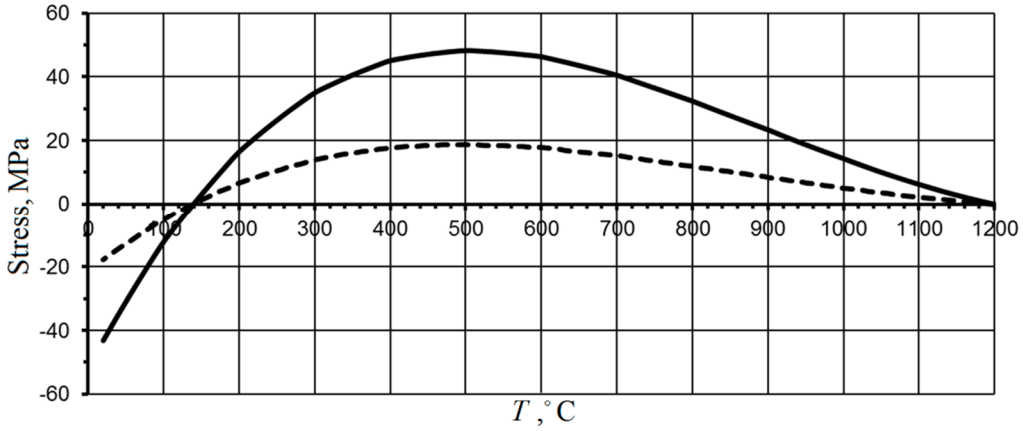

Figure 9. *Temperature dependence of normal and shear contact stresses in the substrate – a surface system in points D and E, MPa:*
——– normal stress, point D; - - - - – shear stress, point E

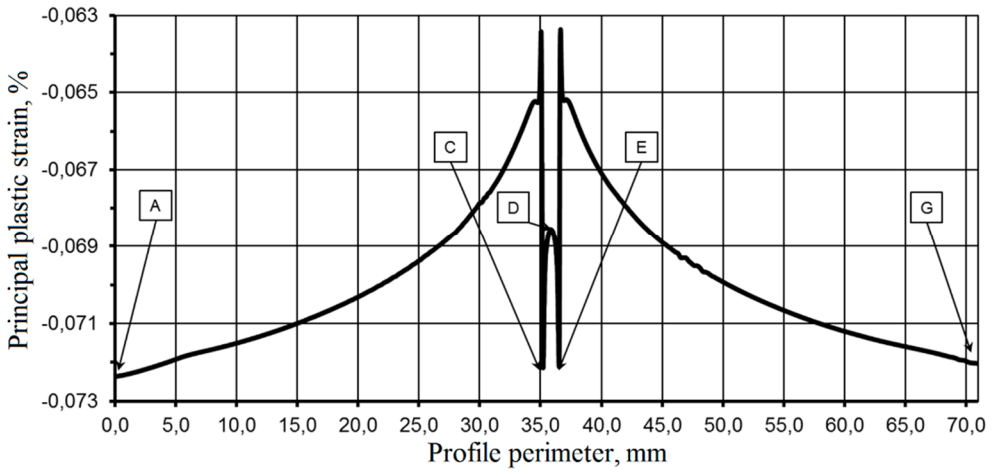

Figure 10. *Distribution of the main plastic deformations in the coating along profile perimeter at $T_к$ = 20°C, %*

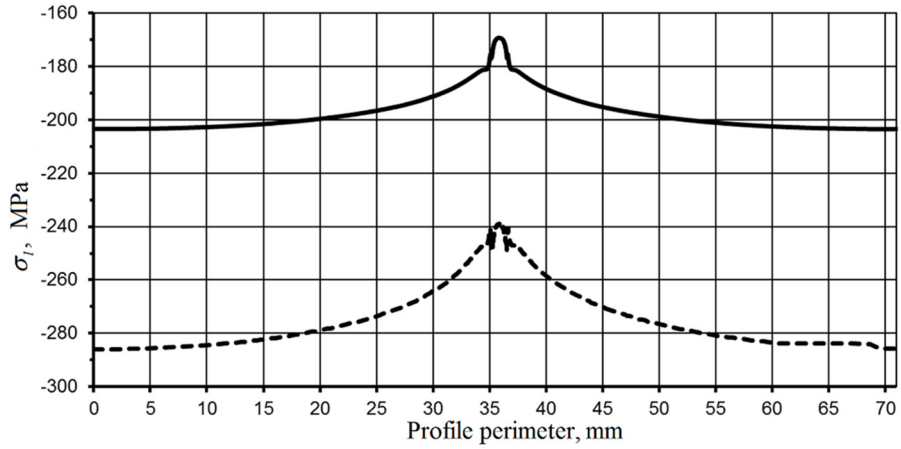

Figure 11. *Coating residual stresses change at the section boundary substrate – coating along the profile perimeter, MPa:*
——– elastic model; - - - - – elastic-plastic model

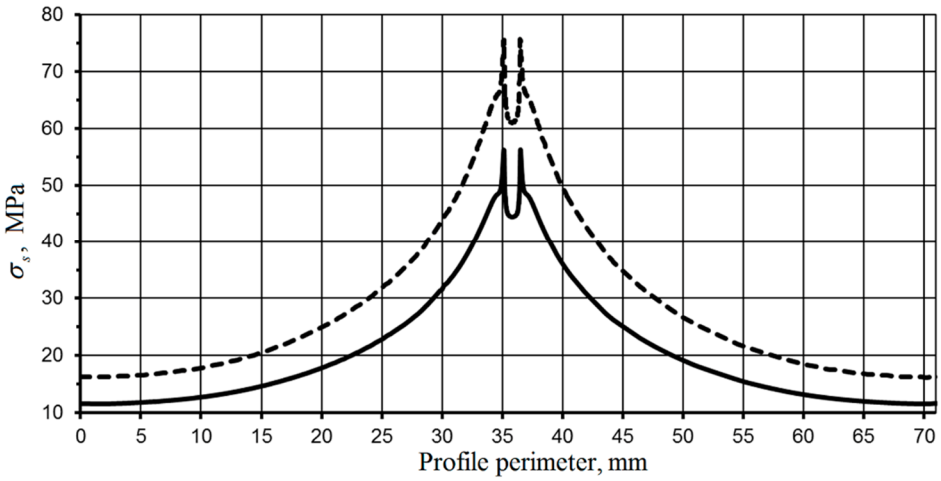

Figure 12. *Substrate residual stresses change at the section boundary substrate – coating along the profile perimeter, MPa:*
——– elastic model; - - - - – elastic-plastic model

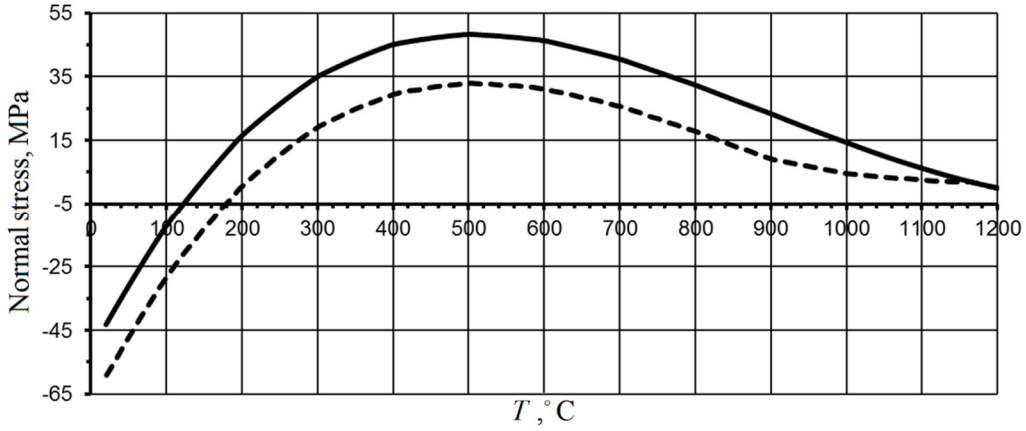

Figure 13. *Temperature dependence of normal contact stresses in the substrate – coating system in the point D, MPa:*
——– elastic model; - - - - – elastic-plastic model

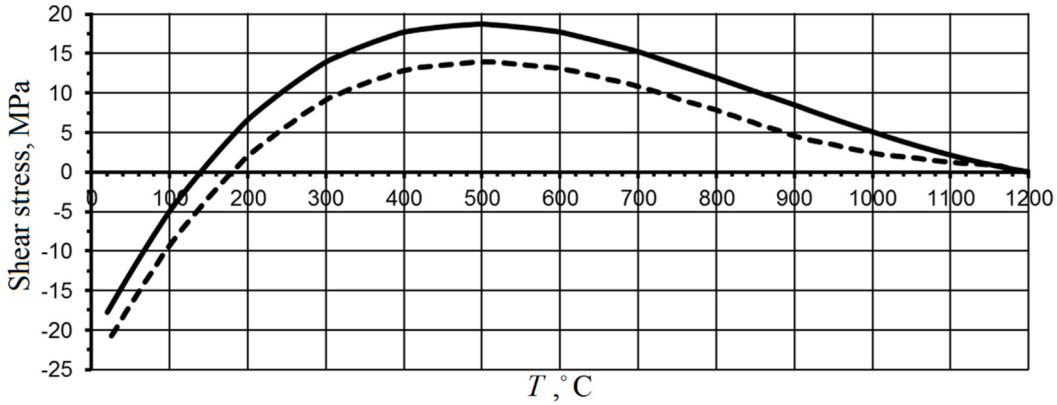

Figure 14. *Temperature dependence of normal contact stresses in the substrate – coating system in the point E, MPa:*
——– elastic model; – – – – elastic-plastic model

Table 1. *Temperature dependencies of structural wall layers material properties and model determination coefficients*

Layers Properties	**ZS6U Substrate**	**Coating SDP-2**	**R^2, substrate / coating**
Modulus of elasticity $E(T)$, MPa	$-138{,}71 \cdot T + 270760$	$-0{,}018 \cdot T^2 - 6{,}155 \cdot T + 162810$	0,949 / 0,993
Poisons ratio $\nu(T)$	$3 \cdot 10^{-8} \cdot T^2 + 3 \cdot 10^{-6} \cdot T + 0{,}313$	$3 \cdot 10^{-8} \cdot T^2 - 1 \cdot 10^{-6} \cdot T + 0{,}3168$	0,974 / 0,981
Tensile strain at break $\delta(T)$, %	-	$0{,}537 \cdot e^{0{,}0053 \cdot T}$	- / 0,959
Yield offset $\sigma_{0,2}(T)$, MPa	$-9 \cdot 10^{-4} \cdot T^2 + 0{,}3575 \cdot T + 950{,}48$	$\begin{cases} 526{,}42 \cdot T^{-0{,}1321}, & T \le 700^\circ\text{C}; \\ 2 \cdot 10^{21} \cdot T^{-6{,}6848}, & 700^\circ\text{C} < T \le 1200^\circ\text{C} \end{cases}$	0,959 / $\begin{cases} 0{,}984; \\ 0{,}999 \end{cases}$
Strength $\sigma_b(T)$, MPa	-	$-1{,}4326 \cdot T + 1541{,}1$	- / 0,923
CLE $\alpha(T) \cdot 10^6$, 1/°C	$7 \cdot 10^{-6} \cdot T^2 - 0{,}0006 \cdot T + 11{,}833$	$10{,}941 \cdot e^{0{,}0006 \cdot T}$	0,929 / 0,953